This is the author version of the work. There may be differences between this version and the published version. You are advised to consult the published version if you wish to cite from it:
https://doi.org/10.1109/LCOMM.2023.3339969

https://eprints.gla.ac.uk/310041/

Deposited on 28 November 2023

Exploiting Multi-Hop RIS-Assisted UAV Communications: Performance Analysis

Mohammad Abualhayja'a, *Student Member, IEEE,* Anthony Centeno, Lina Mohjazi, *Senior Member, IEEE,*
M. Majid Butt, *Senior Member, IEEE,* Philippe Sehier, and Muhammad Ali Imran, *Fellow, IEEE.*

Abstract—Future wireless communication networks are expected to extensively utilise unmanned aerial vehicles (UAVs) and reconfigurable intelligent surfaces (RISs) to improve performance, extend coverage, and enhance energy efficiency. In this paper, the fundamental limits of the system performance of a multi-hop RIS-assisted UAV communication system are analysed and characterised. We derive accurate closed-form approximations for the statistical distributions of the RIS-assisted channels which are then exploited to derive an analytical expression for the signal-to-noise ratio (SNR), outage probability, and bit error rate (BER). Moreover, we derive outage probability expressions in the high SNR regime. Our analysis demonstrates that strategically placing RIS with an adequate number of elements can effectively enhance the performance of UAV communications in different fading scenarios. RIS dynamically adapts to changing channels and user positions, enhancing performance as the UAV navigates diverse geographical areas, when ideal Line of Sight (LoS) conditions may not be consistently attainable due to the UAV's altitude and dynamic mobility.

Index Terms—Reconfigurable intelligent surfaces, unmanned aerial vehicle, outage probability, bit error rate.

I. INTRODUCTION

Due to their distinct characteristics of mobility and flexibility, unmanned aerial vehicles (UAVs) have become key enabler for many applications in wireless communications. The deployment of UAV nodes requires reconfiguring conventional terrestrial networks to tackle challenges, such as dynamic positioning, extensive mobility, and the diverse characteristics of the UAV channels [1]. Reconfigurable intelligent surfaces (RISs) can be exploited in UAV communications and improve the overall performance of UAV communications [2].

Several researchers proposed frameworks to investigate the deployment of RIS in UAV communications. In [2], the authors proposed an optimisation framework for trajectory design and passive beamforming to maximise data rates of a RIS-assisted UAV communications system. In our previous work in [3], we proposed an analytical framework to characterise the outage probability performance of RIS-assisted UAV networks taking into consideration two implementation scenarios, namely, i) UAV serving as an aerial base station (BS) and ii) UAV functioning as an aerial user equipment (UE). We examined the impact of the number of RIS elements and UAV altitude on the outage performance. Our study in

M. Abualhayja'a, A. Centeno, L. Mohjazi, and M. A. Imran are with the James Watt School of Engineering, University of Glasgow, Glasgow, G12 8QQ, UK (e-mail: m.abualhayjaa.1@research.gla.ac.uk, {anthony.centeno, lina.mohjazi, muhammad.imran}@glasgow.ac.uk).

M. Majid Butt is with Nokia, 2000 Lucent Lane, 90563 Naperville, IL, US. (e-mail: majid.butt@nokia.com).

Philippe Sehier is with Nokia, Nokia Bell Labs, 91620 Paris, France (e-mail: philippe.sehier@nokia.com).

[3] also focused on the development of channel models and fading parameters that consider the unique characteristics of UAV communication. Considering a dual-hop RIS-assisted UAV communication system, with the assumption that the UAV serves as a relay to extend the coverage of a ground source node, the work in [4] proposed a performance analysis framework to investigate the outage probability, bit error rate (BER), and average capacity of the system under study. While the findings of this work are useful for understanding the impact of the RIS on the performance of UAV communication networks, they do not offer practical design insights. This stems from the fact that the framework in [4] is based on the assumption that the link between the source and the RIS undergoes Rayleigh fading, and hence, a LoS component does not exist. Nonetheless, it is widely known in the literature on RIS, such as the study in [5], that the RIS attains its highest channel gain when positioned in close proximity to either the source or the destination, and hence, increasing the likelihood of establishing a link with a LoS component between the RIS and the source. Additionally, the derived BER expression in [4] is useful to examine the BER performance for one modulation scheme only, rendering the use of this expression to be limited.

This work explores a multi-hop RIS-assisted UAV communication system with the UAV serving as a relay node. This setup is particularly suitable for various scenarios, such as rural connectivity, disaster response, urban connectivity enhancement, and temporary events, to improve wireless communication by bridging gaps, extending coverage, mitigating obstacles, and enhancing reliability. Additionally, we consider a more generic fading model where the links are modelled by the generic Nakagami-m distribution, which can be simplified into the Rayleigh distribution, signifying the presence of pure NLoS fading characteristics. Furthermore, a one-to-one mapping between the m parameter and the Rice K factor enables the Nakagami-m distribution to serve as an approximation for the Rice distribution [6]. We also consider a realistic scenario with a direct non-line-of-sight (NLoS) link between the source and the destination for a more general cooperative system. The inclusion of RIS and the utilisation of UAV relays present notable challenges to the analysis due to their distinctive characteristics and operational scenarios when compared to BSs or UEs. These challenges primarily involve the mathematical modelling and analysis techniques employed. An analytical framework that accurately evaluates the coverage probability and the reliability of the proposed system is developed. We start with deriving the channel distributions of the RIS-assisted link using the Laguerre series method and then utilise the approximated SNR distribution to obtain accurate approximations for the system outage probability and
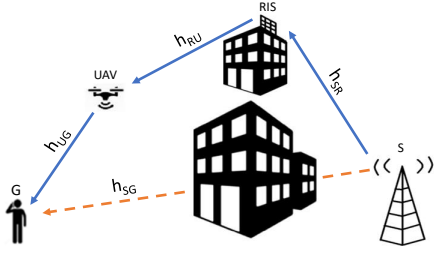
Fig.1. Multi-hop RIS-assisted UAV system model.

BER for generic binary modulation schemes. To gain deeper insights into the system's performance, an asymptotic or high SNR regime analysis of the outage probability is conducted. To the best of our knowledge, this is the first time that the performance of RIS-assisted multi-hop systems operating in composite fading environments with a direct link between the source and destination is examined. The following sections are organised as follows. Section II provides an overview of the system model. In Section III, the SNR outage probability and BER are derived for the proposed systems. Section IV presents the numerical results. Finally, Section V concludes the paper.

II. SYSTEM MODEL

A RIS-assisted multi-hop UAV wireless communication system is shown in Fig.1. We consider the case where a source node (S) is serving a ground user (G) and there is an aerial relay node (U) available to assist in transmission. A RIS (R) equipped with M reflecting elements is positioned atop a building to assist the link between S and U. U receives the signal from S through a RIS-assisted ground-to-air (G2A) link, it then transmits the signal to the ground user using the decode and forward (DF) relaying protocol. In our framework, it is assumed that each node is equipped with a single antenna, and G uses selection combining (SC) to select between signals received from either the direct or the relay links. A time-division channel allocation scheme comprising two time slots is implemented. This configuration enables multiple terminals to collaborate in transmitting to the destination. During the first time slot, source S transmits its signal to both nodes U and G. If the received SNR at node U is above a certain threshold, it decodes the received message and then forwards the source signal to destination D in the second time slot [7]. In this paper, the generic Nakagami-m distribution is adopted as a multipath fading model of S-R and R-U channels. We also assume that the envelope of the direct channel between S and G is modelled as a Rayleigh distribution.

A. G2A RIS-assisted Link

In the first transmission stage, the S transmits the signal to U through the RIS-assisted G2A link. The signal received by the UAV can be written as

$$y_1 = \left[\sum_{i=1}^{M} h_{SR,i} e^{j\varphi_i} h_{RU,i} \right] x_1 + n_1, \quad (1)$$

where $h_{SR,i} = \sqrt{\rho d_{SR}^{-\alpha}} \mu_i e^{-j\epsilon_i}$ and $h_{RU,i} = \sqrt{\rho d_{RU}^{-\alpha}} \zeta_i e^{-j\theta_i}$ represent S-R and R-U links channel gains, respectively, ρ is

the path loss at reference distance of 1m, d_{SR} and d_{RU} are the distances between S-R and R-U, respectively, α is the pathloss exponent, μ and ζ denote the multipath fading coefficients modelled by independent Nakagami-m distributions, φ_i is phase-shift applied by the ith element of the RIS, x_1 is the transmitted signal from S, and $n_1 \sim \mathcal{CN}(0, N_0)$ is the additive white Gaussian noise (AWGN) at U with zero mean and N_0 variance.

From [2], the instantaneous SNR can be maximised by aligning the phases of the signals at U, i.e., $\varphi = \epsilon + \theta$, therefore, from (1), the maximum instantaneous SNR at U can be written as

$$\gamma_{SU} = \frac{P_1 (\sum_{i=1}^{M} h_{SR,i} h_{RU,i})^2}{N_0} = \bar{\gamma}_1 X_1^2, \quad (2)$$

where P_1 is the transmit power, $\bar{\gamma}_1 = \frac{P_1}{N_0}$ is the average transmit SNR, and $X_1 = \sum_{i=1}^{M} h_{SR,i} h_{RU,i}$. It can be noticed that X_1 is the sum of M double Nakagami-m independent random variables (RVs). The probability density function (PDF) of double Nakagami-m is expressed as [8]

$$f_{Y_i}(\gamma) = \frac{4\gamma^{m_1 + m_2 - 1}}{\prod_{\ell=1}^{2} \Gamma(m_\ell)(\Omega_\ell/m_\ell)^{(m_1 + m_2)/2}} \times K_{m_1 - m_2} \left(2\gamma \prod_{i=1}^{2} \sqrt{\frac{m_i}{\Omega_\ell}} \right), \quad (3)$$

where $\Gamma(\cdot)$ is the gamma function, Ω_l is the average fading power, m_l is the shape parameter, and $K_\nu(\cdot)$ is the νth-order modified Bessel function of the second kind.

The nth-order moment of the RV Y_i, can be given by [8]

$$\mathbb{E} \langle Y_i^n \rangle = \prod_{\ell=1}^{2} \frac{\Gamma(m_\ell + n/2)}{\Gamma(m_\ell)} \left(\frac{\Omega_\ell}{m_\ell} \right)^{n/2}. \quad (4)$$

Since $\mathbb{E} \langle Y_i^n \rangle$ is a linear operator, implying that $E(X_1) = M(E(Y_i))$ holds true. Additionally, assuming that Y_i is independent for all values of i, then $Var(X_1) = M(Var(Y_i))$.

Using the first term of a Laguerre series, PDF of X_1 can be tightly approximated as follows [9]

$$f_{\gamma_{SU}}(\gamma) = \frac{1}{b\Gamma(a+1)} \left(\frac{\gamma}{b} \right)^a \exp \left[-\frac{\gamma}{b} \right], \quad (5)$$

where $a = \frac{(E(X_1))^2}{\text{Var}(X_1)} - 1$ and $b = \frac{\text{Var}(X_1)}{E(X_1)}$ are parameters defined through the mean and the variance of X_1.

B. A2G link

In the second relay transmission phase, U sends the decoded signal to G. The received signal at G can be represented as

$$y_2 = h_{UG} x_2 + n_2, \quad (6)$$

where $h_{UG} = \sqrt{\rho d_{UG}^{-\alpha}} \beta e^{-j\Psi}$ is the channel gain for the U-G link, d_{UG} is the distances between the nodes U-G, β denote the multipath fading coefficient modelled as an independent Nakagami-m distribution, x_2 is the transmitted signal from the UAV, and $n_2 \sim \mathcal{CN}(0, N_0)$ is the AWGN at G with zero mean and N_0 variance.

From (6), the SNR of the U-G link can be given by

$$\gamma_{UG} = \frac{P_2 |h_{UG}|^2}{N_0} = \bar{\gamma}_2 X_2^2, \quad (7)$$

where P_2 is the transmit power of U, $\overline{\gamma}_2 = \frac{P_2}{N_0}$ is the average transmit SNR, and X_2 is modelled by an independent Nakagami-m RV. From [6], the PDF of X_2 can be expressed as

$$f_{\gamma_{UG}}(\gamma) = \frac{2m_3^{m_3}}{\Gamma(m_3)\Omega_3^{m_3}}\gamma^{2m_3-1}\exp\left(-\frac{m_3}{\Omega_3}\gamma^2\right), \quad (8)$$

where $\Gamma(\cdot)$ is the gamma function, Ω_3 is the average fading power, and m_3 is the shape parameter.

C. Direct Link

In addition to the dual-hop cascaded link, we assume to have a NLoS link between S and G. The direct signal received by the user can be represented as

$$y_D = h_{SG}x_1 + n_3, \quad (9)$$

where $h_{SG} = \sqrt{\rho d_{SG}^{-\alpha}}\upsilon e^{-j\kappa}$ is the channel gain for S-G link, d_{SG} is the distances between the nodes U-G, υ denotes the multipath fading coefficient modelled as an independent Rayleigh distribution, and $n_3 \sim \mathcal{CN}(0, N_0)$ is the AWGN at G with zero mean and N_0 variance. Hence, the SNR of the direct link can be expressed as

$$\gamma_{SG} = \frac{P_1|h_{SG}|^2}{N_0} = \overline{\gamma}_1 X_D^2, \quad (10)$$

where X_D is modelled by an independent Rayleigh RV. From [6], the PDF of X_D can be given by

$$f_{\gamma_{SG}}(\gamma) = \frac{\gamma}{\sigma^2}e^{-\gamma^2/(2\sigma^2)}, \quad (11)$$

where σ is the scale parameter of the distribution.

III. PERFORMANCE ANALYSIS

This section focuses on evaluating the performance of the proposed system by analysing the outage probability and BER.

A. Outage Probability

With SC, the destination terminal selects the signal with the largest received SNR. The instantaneous end-to-end SNR at G can then be expressed as

$$\gamma_{SC} = \max_{j\in direct,relay}\gamma_j, \quad (12)$$

where γ_j is the jth path received signal SNR.

The outage probability corresponds to the probability that the system fails to meet a desired threshold SNR, γ_{th}. Hence, the end-to-end outage probability can be written as

$$P_{\text{out}} = \Pr[\gamma_{sc} < \gamma_{th}]. \quad (13)$$

Since the γ_j's are independent, the outage probability can be expressed as [10]

$$P_{\text{out}} = \prod_{j\in direct,relay}\Pr[\gamma_j < \gamma_{th}]. \quad (14)$$

Assuming a DF protocol at the aerial relay node, an outage occurs when either one of the links is in outage. According,

the outage probability for the relay-assisted transmission can be written as

$$P_{\text{out},relay} = 1 - (1 - P_{\text{out},SU})(1 - P_{\text{out},UG}). \quad (15)$$

Similar to [11], from (5) the outage probability at the UAV for S-U RIS-assisted link can be given by

$$P_{\text{out},SU} = \Pr[\gamma_{SU} < \gamma_{th}] = \frac{\gamma\left(a+1, \frac{\sqrt{\gamma_{th}}}{b\sqrt{L_1\overline{\gamma}_1}}\right)}{\Gamma(a+1)}, \quad (16)$$

where $\gamma(\cdot,\cdot)$ is the lower incomplete gamma function and $L_1 = \rho^2(d_{SR}^{-\alpha})(d_{RU}^{-\alpha})$.
From (8), $P_{\text{out},UG}$ can be given by

$$P_{\text{out},UG} = \Pr[\gamma_{UG} < \gamma_{th}] = \frac{\gamma\left(m_3, \frac{m_3\gamma_{th}}{\Omega_3 L_2\overline{\gamma}_2}\right)}{\Gamma(m_3)}, \quad (17)$$

where $L_2 = \rho d_{UG}^{-\alpha}$.

It can be seen that P_{out} of the RIS-assisted link is a decreasing function of the square root of the transmission SNR and the path loss between nodes. This suggests that the RIS-assisted link may exhibit better robustness to variations in these parameters compared to the U-G link.
Finally, the outage probability of the direct link can be obtained as

$$P_{\text{out},SG} = \Pr[\gamma_{SG} < \gamma_{th}] = 1 - e^{-\gamma_{th}/(2\sigma^2\overline{\gamma}_1 L_3)}, \quad (18)$$

where $L_3 = \rho d_{SG}^{-\alpha}$.

Here, we derive a closed-form expression for the outage probability in the high SNR regime to provide further context for the system performance.
At high SNR ($\gamma \to \infty$), the outage performance of the relay-assisted transmission can be asymptotically written as

$$P_{\text{out},relay} \to P_{\text{out},SU}^A + P_{\text{out},UG}^A. \quad (19)$$

By exploiting [18, eq. (8.354.1)], $P_{\text{out},SU}$ can be evaluated at high SNR values as

$$P_{\text{out},SU}^\infty \simeq \frac{\sum_{n=0}^{\infty}\frac{(-1)^n\left(\sqrt{\frac{\gamma_{th}}{\overline{\gamma}_1}}\right)^{a+n+1}}{(a+n+1)b^{a+n+1}}}{\Gamma(a+1)}. \quad (20)$$

The initial term in the summation presented in (20) significantly outweighs the remaining terms. Hence, after considering that term only and with some simple mathematical manipulations, (20) simplifies to

$$P_{\text{out},SU}^\infty \simeq \left[\frac{b^2}{\gamma_{th}\left[(a+1)!\right] - \frac{2}{(a+1)}}\overline{\gamma}_1\right]^{-\frac{(a+1)}{2}}. \quad (21)$$

The asymptotic outage probability over Nakagami-m channels can be evaluated as [12]

$$P_{\text{out},UG} \approx \frac{m_3^{m_3-1}}{\Gamma(m_3)}\left(\frac{\gamma_{th}}{\overline{\gamma}_2}\right)^{m_3}. \quad (22)$$

Similarly, the asymptotic outage probability for the direct channel over the Rayleigh fading can be given by [12]

$$P_{\text{out},SG} \approx \frac{\gamma_{\text{th}}}{\bar{\gamma_1}}. \qquad (23)$$

B. BER Analysis

The unified unconditional average BER expression for SC communication and arbitrary binary modulation schemes is given by [13]

$$P_{BER} = \frac{q^p}{2\Gamma(p)} \int_0^\infty e^{-q\gamma} \gamma^{p-1} F_{\gamma_{sc}}(\gamma) \, d\gamma, \qquad (24)$$

where p and q are modulation scheme related parameters [4]. From (14) and (15), $F_{\gamma_{sc}}(\gamma)$ can be given by

$$F_{\gamma_{sc}}(\gamma) = (F_{\gamma_{SU}}(\gamma) + F_{\gamma_{UG}}(\gamma) - F_{\gamma_{SU}}(\gamma) F_{\gamma_{UG}}(\gamma)) \\ \times F_{\gamma_{SG}}(\gamma), \qquad (25)$$

where $F_{\gamma_{SU}}$, $F_{\gamma_{UG}}$, and $F_{\gamma_{SG}}$ are the cumulative distribution functions of γ_{SU}, γ_{UG}, and γ_{SG}, respectively. Hence, the integral at (24) becomes an integral of three terms as follows

$$P_{BER} = \frac{q^p}{2\Gamma(p)}(I_1 + I_2 - I_3), \qquad (26)$$

where,

$$I_1 = \int_0^\infty e^{-q\gamma} \gamma^{p-1} F_{\gamma_{SU}}(\gamma) F_{\gamma_{SG}}(\gamma) \, d\gamma, \qquad (27)$$

$$I_2 = \int_0^\infty e^{-q\gamma} \gamma^{p-1} F_{\gamma_{UG}}(\gamma) F_{\gamma_{SG}}(\gamma) \, d\gamma, \qquad (28)$$

and

$$I_3 = \int_0^\infty e^{-q\gamma} \gamma^{p-1} F_{\gamma_{SU}}(\gamma) F_{\gamma_{UG}}(\gamma) F_{\gamma_{SG}}(\gamma) \, d\gamma. \qquad (29)$$

The integral I_1 can be solved through integration by substitution followed by exploiting [14, Eq.(2.10.3.9)] to derive the expression of (30), shown at the bottom of this page.
where $_aF_b(.)$ is the confluent hypergeometric function [14]. The integral I_2 can be evaluated by applying [14, Eq.(2.10.3.2)] to obtain

$$I_2 = \frac{\Gamma(p+m_3)(\frac{m_3}{\Omega_3 L_2 \bar{\gamma_2}})^{m_3}}{m_3 \Gamma(m_3) q^{(p+m_3)}} \\ \times {}_2F_1\left(m_3, p+m_3; m_3+1; -\frac{(\frac{m_3}{\Omega_3 L_2 \bar{\gamma_2}})}{q}\right). \qquad (31)$$

The third integral term contains two lower incomplete gamma functions with different arguments which makes it difficult to evaluate. To overcome this, a series representation of the lower incomplete gamma function is used to replace the $F_{\gamma_{SU}}(\gamma)$ term, resulting in

$$F_{\gamma_{SU}}(\gamma) = \frac{1}{\Gamma(a+1)} \sum_{k=0}^\infty \frac{(-1)^k (\frac{\sqrt{\gamma_{th}}}{b\sqrt{L_1 \bar{\gamma_1}}})^{k+a+1}}{k!(a+k+1)}. \qquad (32)$$

After some mathematical manipulations the integral I_3 can be rewritten as

$$I_3 = \frac{1}{\Gamma(a+1)} \sum_{k=0}^\infty \frac{-1^k (b\sqrt{L_1 \bar{\gamma_1}})^{-(k+a+1)}}{k!(k+a+1)\Gamma(m3)} \\ \times \int_0^\infty e^{-q\gamma} \gamma^{\frac{p+k+a-1}{2}} \gamma\left(m_3, \frac{m_3 \gamma_{th}}{\Omega_3 L_2 \bar{\gamma_2}}\right) d\gamma, \qquad (33)$$

which consists of a sum of integrals of the form given in [14, Eq.(2.10.3.2)]. Consequently, I_3 can be evaluated as in (34), shown at the bottom of this page.

IV. NUMERICAL AND SIMULATION RESULTS

This section presents numerical findings aimed at gaining insights into the impact of the RIS size and UAV positioning (altitude) on the performance of the system. To verify our analysis, MATLAB is employed to generate Monte Carlo simulation by using 10^8 realisations, and the following simulation parameters: $P_1 = P_2 = 49$ dBm, $\rho = -1$ dB, $N_0 = -110$ dBm, $\alpha = 3.5$ and 2.8 for S-G and S-R links, respectively, and 2.2 for both R-U and U-G links. The horizontal distances S-R, R-U, U-G, and S-G are 70, 320, 60 and 320 m, respectively.

Fig. 2(a) shows end-to-end outage probability as a function of the UAV height with respect to the ground. The analytical results are consistent with the simulations, which demonstrates the accuracy of the proposed approximation. Furthermore, The outage probability of the multi-hop system demonstrates a

$$I_1 = \frac{1}{\Gamma(a+1)} \left(\frac{\left(\left(\frac{1}{b\sqrt{L_1 \gamma_1}}\right)^{a+1}\right)}{2(a+1)} q^{-(2p+a+1)/2} \Gamma\left(\frac{2p+a+1}{2}\right) {}_2F_2\left(\frac{a+1}{2}, \frac{2p+a+1}{2}; \frac{1}{2}, \frac{a+1}{2}+1 : \frac{\left(\frac{1}{b\sqrt{L_1 \gamma_1}}\right)^2}{4q}\right) \right.$$
$$\left. + \frac{\left(\frac{1}{b\sqrt{L_1 \gamma_1}}\right)^{a+2}}{2(a+2)} q^{-(2p+a+2)/2} \Gamma\left(\frac{2p+a+2}{2}\right) {}_2F_2\left(\frac{a+2}{2}, \frac{2p+a+2}{2}; \frac{3}{2}, \frac{a+4}{2} : \frac{\left(\frac{1}{b\sqrt{L_1 \gamma_1}}\right)^2}{4q}\right) \right). \qquad (30)$$

$$I_3 = \sum_{k=0}^\infty \frac{-1^k (b\sqrt{L_1 \bar{\gamma_1}})^{-(k+a+1)}}{k!(k+a+1)\Gamma(a+1)} \frac{\Gamma(\frac{2p+k+a+1}{2}+m_3)(\frac{m_3}{\Omega_3 L_2 \bar{\gamma_2}})^{m_3}}{m_3 \Gamma(m_3) q^{(\frac{2p+k+a+1}{2}+m_3)}} \times {}_2F_1\left(m_3, \frac{2p+k+a+1}{2}+m_3; m_3+1; -\frac{(\frac{m_3}{\Omega_3 L_2 \bar{\gamma_2}})}{q}\right). \qquad (34)$$
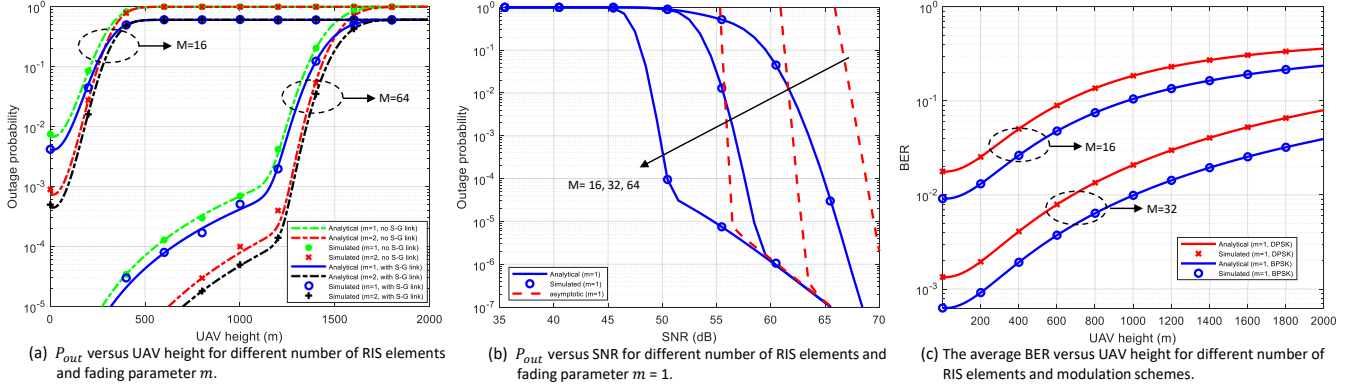
Fig.2. P_{out} and average BER for different numbers of RIS elements and fading parameters.

noteworthy enhancement with the increase in the size of RIS. Thus, a sufficiently high number of RIS elements ensures a reliable connection between S and U, hence, in that case, the outage of the system is mainly determined by A2G link. This result is particularly useful for design considerations, where for the UAV operating at a specific height, a certain number of RIS elements are used to reach a desired performance and vice versa. Our investigation yields an additional noteworthy insight, indicating that a RIS with a sufficient size can maintain a reliable link between S and U when U moves closer to G.

The system's outage performance, represented in Fig. 2(b), is evaluated in relation to the transmit SNR for various numbers of RIS elements. The analytical results closely match the simulation findings, demonstrating the consistency of the proposed analysis. A noteworthy observation is that the performance of the system with a larger RIS closely resembles the high SNR performance of the system with a smaller RIS. For instance, when comparing a RIS with 64-elements to an 16-element RIS, it is observed that the former achieves a similar outage performance at a transmit SNR of 50 dB as the latter does at an SNR of 65 dB indicating that employing a larger RIS can attain energy-efficient and reliable connections to meet the demands of diverse propagation environments. It is also worth noting that the high SNR asymptotic behaviour aligns with the exact results.

Fig.2(c) represents end-to-end BER different modulation schemes as a function of the UAV height. As expected, the simulation matches the analytical results. Moreover, the series expansion used to replace the lower incomplete gamma function in (32) converges for the given parameter values. It can be clearly seen that a RIS with a sufficient size can stabilise the performance and maintain a reliable connection, and the behaviour of the average BER performance is similar to the outage performance behaviour.

V. CONCLUSION

This study presents a framework to examine the performance of RIS-assisted UAV communications. Closed-form accurate approximations for the SNR distribution of the RIS-assisted UAV networks over Nakagami-m fading channels, outage probability, and average BER for the proposed system were derived. These expressions were exploited to evaluate

the outage and error performance of the proposed systems. Furthermore, high SNR outage probability expressions were also derived and analysed. These results highlight the effectiveness of RIS in optimising system performance according to specific requirements or constraints. Our study shows that the integration of RIS presents an efficient solution, particularly in complex and dynamic environments where maintaining LoS connections might not always be feasible or optimal.

REFERENCES

[1] Y. Zeng, J. Lyu, and R. Zhang, "Cellular-Connected UAV: Potential, Challenges, and Promising Technologies," *IEEE Wirel. Commun.*, vol. 26, no. 1, pp. 120–127, Sep. 2018.
[2] S. Li *et al.*, "Reconfigurable Intelligent Surface Assisted UAV Communication: Joint Trajectory Design and Passive Beamforming," *IEEE Wireless Commun. Lett.*, vol. 9, no. 5, pp. 716–720, Jan. 2020.
[3] M. Abualhayja'a *et al.*, "On the outage performance of reconfigurable intelligent surface-assisted uav communications," in *2023 IEEE WCNC*, March 2023, pp. 1–6.
[4] L. Yang *et al.*, "On the Performance of RIS-Assisted Dual-Hop UAV Communication Systems," *IEEE Trans. Veh. Technol*, vol. 69, no. 9, pp. 10 385–10 390, Jun. 2020.
[5] Q. Wu *et al.*, "Intelligent Reflecting Surface-Aided Wireless Communications: A Tutorial," *IEEE Trans. Commun.*, vol. 69, no. 5, pp. 3313–3351, Jan. 2021.
[6] M. Simon and M.-S. Alouini, *Digital Communication Over Fading Channels*, 2nd ed. Hoboken, NJ, USA: Wiley, 2005.
[7] J. Laneman and G. Wornell, "Distributed space-time-coded protocols for exploiting cooperative diversity in wireless networks," *IEEE Trans. Inf. Theory*, vol. 49, no. 10, pp. 2415–2425, 2003.
[8] G. K. Karagiannidis *et al.*, "$n*$nakagami: A novel stochastic model for cascaded fading channels," *IEEE Trans. Commun.*, vol. 55, no. 8, pp. 1453–1458, Aug. 2007.
[9] S. Primak, V. Kontorovich, and V. Lyandres, *Stochastic methods and their applications to communications: stochastic differential equations approach*. John Wiley & Sons, Aug. 2005.
[10] J. Hu and N. C. Beaulieu, "Performance analysis of decode-and-forward relaying with selection combining," *IEEE Commun. Lett.*, vol. 11, no. 6, pp. 489–491, 2007.
[11] A. M. Salhab and M. H. Samuh, "Accurate Performance Analysis of Reconfigurable Intelligent Surfaces Over Rician Fading Channels," *IEEE Wireless Commun. Lett.*, vol. 10, no. 5, pp. 1051–1055, Feb. 2021.
[12] Z. Wang and G. Giannakis, "A simple and general parameterization quantifying performance in fading channels," *IEEE Trans. Commun.*, vol. 51, no. 8, pp. 1389–1398, Aug. 2003.
[13] I. S. Ansari *et al.*, "A new formula for the BER of binary modulations with dual-branch selection over generalized-k composite fading channels," *IEEE Transactions on Communications*, vol. 59, no. 10, pp. 2654–2658, Jul. 2011.
[14] A. Prudinikov, Y. Brychkov, and O. Marichev, *Integrals and series: special functions*. New York, NY, USA: Gordon and Breach (Publishers, Inc.), 1992, vol. 2.